Supporting Information

Fungal siderophore biosynthesis catalysed by an iterative nonribosomal peptide synthetase

Yang Hai,[1‡] Matthew Jenner, *[3,4] and Yi Tang*[1,2]

[1]Department of Chemical and Biomolecular Engineering and [2]Department of Chemistry and Biochemistry, University of California, Los Angeles, California 90095, United States. [3]Department of Chemistry, University of Warwick, Coventry, UK. [4]Warwick Integrative Synthetic Biology (WISB) Centre, University of Warwick, Coventry, UK.

[‡]Present address: Department of Chemistry and Biochemistry, University of California, Santa Barbara, Santa Barbara, California, 93106, United States.

*Correspondence: m.jenner@warwick.ac.uk, yitang@ucla.edu

Table of Contents

1. Materials and Methods 4
1.1. Chemicals and general methods 4
1.2. Protein heterologous expression and purification 4
1.3. Genetic manipulation 5
1.4. Siderophore isolation and amino acid substrate preparation 5
1.5 Biochemical characterization of SidD *in vitro*. 5
1.6 UHPLC-ESI-Q-TOF-MS analysis of intact proteins 6
2. Figures. 7
Figure S1. SDS-PAGE analysis of purified SidD and related variants used in this study. 7
Figure S2. Mass spectrum of FSC (1) from LC-MS analysis of SidD in vitro reaction. 8
Figure S3. Mass spectrum of Fe-FSC Fe-(1) from LC-MS analysis of SidD in vitro reaction. 8
Figure S4. Mass spectrum of Linear-FSC (3) from LC-MS analysis of SidD in vitro reaction. 9
Figure S5. Mass spectrum of Linear-Fe-FSC Fe-(3) from LC-MS analysis of SidD *in vitro* reaction. 9
Figure S6. Mass spectrum of tetra-*cis*-AMHO (4) from LC-MS analysis of SidD *in vitro* reaction. 10
Figure S7. High resolution MS/MS mass spectrum of tetra-*cis*-AMHO (4) from LC-MS analysis of SidD *in vitro* reaction. 11
Figure S8. Mass spectrum of Fe-tetra-*cis*-AMHO Fe-(4) from LC-MS analysis of SidD *in vitro* reaction. 12
Figure S9. High resolution MS/MS mass spectrum of Fe-tetra-*cis*-AMHO (4) from LC-MS analysis of SidD *in vitro* reaction. 13
Figure S10. HPLC traces showing degradation of AMHO (1) to N^5-hydroxy-L-ornithine and Δ^2-anhydro-mevalonate lactone (2) under acidic conditions. 14
Figure S11. Possible mechanisms for spontaneous intermediate offloading to give 3. 15
Figure S12. Plausible mechanisms for intermodular T domain loading. 16
Figure S13. Biosynthetic assembly of *cis*-AMHO units by SidD(ΔC_T). 17
Figure S14. Proposed biosynthetic route to FSC (1) using the 'back transfer' approach. 18
Figure S15. Proposed biosynthetic pathway for coprogen. 19
Figure S16. ^{1}H-NMR spectrum of AMHO in CD_3OD. 20
Figure S17. ^{13}C-NMR spectrum of AMHO in CD_3OD. 21
Figure S18. ^{1}H-^{1}H COSY-NMR spectrum of AMHO in CD_3OD. 22
Figure S19. HSQC-NMR spectrum of AMHO in CD_3OD. 23
Figure S20. HMBC-NMR spectrum of AMHO in CD_3OD. 24
Figure S21. Gene-knockout of *sidG* in *A. nidulans*. 25
3. Tables 26
Table S1. Plasmid maps of wild-type constructs used in this study. 26
Table S2. Oligonucleotides used for cloning and mutagenesis in this study. 27

Table S3. ^{1}H and ^{13}C NMR chemical shifts of AMHO measured in CD_3OD. The numbered structure of AMHO is shown for reference. 28

Table S4. Amino acid sequences of wild-type SidD protein and other SidD constructs used in this study. 29

Table S5. Calculated and measured mass values for species detected using intact protein mass spectrometry.. 32

1. Materials and Methods

1.1. Chemicals and general methods

Triacetylfusarinine C (TAFC), desferri-triacetylfusarinine C, fusarinine C (FSC), and desferri-fusarinine C were purchased from EMC microcollections, Germany. Isopropyl β-D-1-thiogalacopyranoside (IPTG) was purchased from Gold Biotechnology. All other chemicals were purchased from Fisher. PCR reactions were performed using the Phusion® high-fidelity DNA polymerase (New England Biolabs) according to the manufacturer's instructions. cDNA was synthesized by using the SuperScript® II Reverse Transcriptase Kit (Life Technologies). Custom oligonucleotides were synthesized by Integrated DNA Technologies. *Escherichia coli* strain DH10B strain was used for cloning procedures. NMR spectra were recorded on a Bruker AV500 spectrometer equipped with a cryo-probe. The HR-MS data were recorded on an Agilent 6545 Q-TOF LC-MS.

1.2. Protein heterologous expression and purification

The SidD (AFUA_3G03420) gene exon fragments were cloned from the genomic DNA extract of *A. fumigatus ku80* strain.[1] The corresponding yeast expression plasmids were assembled through yeast homologous recombination using a Frozen-EZ Yeast Transformation II Kit (Zymo research). Gene fragments were integrated into a 2μ-based yeast expression vector with auxotrophic markers and ADH2 promoter and terminator (plasmid maps see Table S1). To facilitate purification, SidD was fused with an *N*-terminal octahistidine tag. The full-length proteins were expressed in *S. cerevisiae* JHY686 strain cultured in YPD medium. Briefly, single colonies of yeast cells harboring expressing plasmids was inoculated into SDCt uracil drop-out culture and left grown at 28 °C for 2days. The seed culture was then inoculated into YPD culture (1 ml to 50 mL) and left grown at 28 °C for another 2 days. Cells were harvested by centrifugation and washed once with cell lysis buffer (50 mM K_2HPO_4 (pH 7.5), 10 mM imidazole, 300 mM NaCl, 5% glycerol). Cells were flash frozen in liquid nitrogen and lysed by using a stainless-steel Waring blender. The cell lysate was cleared by centrifugation at 26,000 g for 60 min at 4 °C and the supernatant was filtered through a 0.22 μm filter (Millipore). The filtrate was incubated with Ni^{2+}-NTA resin for 30 min at 4 °C and then the slurry was loaded onto a gravity column. The resin was washed and eluted with increasing concentrations of imidazole in cell lysis buffer. The fractions were examined by SDS-PAGE gels (Figure S1). Pure fractions were concentrated to 20 mg/mL by Amicon concentrators (Millipore), supplemented with 10% glycerol and stored at -80 °C. Protein concentrations were determined by Bradford assay. Typically, 2 L cell culture could yield 1-10 mg proteins depending on the nature of the protein construct.

For bacterial expression, the target regions were subcloned into a modified pET28a (+) vector (Addgene plasmid #29656). The resulting *N*-terminal TEV protease cleavable hexahistidine tagged individual domains were overexpressed in *E. coli* BL21(DE3) cells in LB medium in the presence of 50 mg/L kanamycin. Expression was induced by 100 μM IPTG when OD_{600} reached 0.8 and the cell cultures were left grown at 16 °C overnight. Cells

were harvested by centrifugation and lysed by sonication. Purification was performed similarly to the full-length protein.

1.3. Genetic manipulation

The *A. nidulans* ΔSidG strain derived from the parent *A. nidulans* ΔEM strain[2] was constructed by integration of a *pyroA* marker to the *SidG* loci (AN8539) through homologous recombination. The integration of marker was selected by dropping out pyridoxin from the growth medium and verified by colony-PCR (**Figure S11**). The resulting strain was fermented to obtain fusigen and desferrifusigen.

1.4. Siderophore isolation and amino acid substrate preparation

The amino acid substrate N^5-*cis*-anhydromevalonyl-N^5-hydroxy-L-ornithine (AMHO) was prepared via ester base hydrolysis of fusarinine C. To prepare Fe-AMHO substrate, 1 mg of commercially available FSC-Fe complex was dissolved in water and the pH was adjusted to 12 with 1 M NaOH. The solution was stirred at room temperature for 15 min and then neutralized with 1 M HCl. The resulting solution was lyophilized and the Fe-AMHO substrate was used without further purification. To prepare Fe-free AMHO, FSC was isolated from the *A. nidulans* ΔSidG strain (see **Section 1.3**) when cultured under the iron-limiting condition (minimal medium containing 1% glucose as the carbon source, 20 mM glutamine as the nitrogen source and 20 μg/L biotin)[3] at 37 °C. The culture filtrate was fractionated with Amberlite XAD-16 (Sigma-Aldrich) resin using a gradient of H_2O/MeOH. Fractions containing FSC were combined and the organic solvent was removed by rotary evaporation. The pH of the aqueous solution was brought up to 12 by addition of 1M NaOH. The solution was stirred at room temperature for 1 hr and then neutralized with 1M HCl. The resulting L-AHMO was further purified by semipreparative HPLC using a reverse-phase column (Phenomenex Kinetics, C18, 5 μm, 100 Å, 250 x 4.6 mm). Ammonium formate 0.1% (w/v) was added to the mobile phase (H_2O/MeCN) as the ion-pairing agent. The identity of AMHO was verified by NMR and HRMS analysis. The NMR spectra data are consistent with the literature data and are summarized in **Table S3**.[4] HRMS: calc. for $[M+H]^+$ $C_{11}H_{21}N_2O_5^+$, 261.1445; found 261.1447.

1.5 Biochemical characterization of SidD *in vitro*.

Purified SidD and associated variants/mutants were converted to their *holo*- form by incubation in 20 mM Tris HCl, 100 mM NaCl, 2 μM of NpgA, 0.1 mM CoA and 10 mM $MgCl_2$ in a total volume of 50 μL for 1 hrs at 25 °C. Reaction was initiated by addition of ATP (5 mM) and AMHO (1 mM) in a final volume of 50 μL, and the reaction was allowed to proceed at 25 °C. At different time points, the reaction was quenched by mixing with equal volume of methanol. The reaction products were analyzed on an UHPLC-MS on a Shimadzu 2020 EVLC–MS (Phenomenex kinetex, 1.7 μm, 2.0 x 100 mm, C18 column) using positive and negative mode electrospray

ionization with a linear gradient of 5−95% MeCN−H_2O supplemented with 0.1% (v/v) formic acid in 15 min followed by 95% MeCN for 5 min with a flow rate of 0.3 mL/min.

For steady-state kinetics, 1 μM of *holo*-SidD was used in the assay and the reaction was quenched after 5 min by mixing with equal volume of methanol. To convert desferri-FSC into ferri-FSC, 1 mM $FeCl_3$ was added to the reaction mixture and the product was quantified by HPLC. An external standard curve was made by using commercially available ferri-FSC standard.

1.6 UHPLC-ESI-Q-TOF-MS analysis of intact proteins

Purified SidD and associated mutants were converted to their *holo*- form as described above, except that Sfp enzyme was used and the incubation time was 3 hrs. Loading of AMHO was initiated by addition of ATP (5 mM) and AMHO (1 mM) in a final volume of 50 μL, and the loading reaction was allowed to proceed for 15 min or 1 hr at 25 °C before intact protein analysis by UHPLC-ESI-Q-TOF-MS.

Enzymatic assays were analyzed on a Bruker MaXis II ESI-Q-TOF-MS connected to a Dionex 3000 RS UHPLC fitted with an ACE C4-300 RP column (100 x 2.1 mm, 5 μm, 30 °C). The column was eluted with a linear gradient of 5–100% MeCN containing 0.1% formic acid over 30 min. The mass spectrometer was operated in positive ion mode with a scan range of 200–3000 m/z. Source conditions were: end plate offset at −500 V; capillary at −4500 V; nebulizer gas (N_2) at 1.8 bar; dry gas (N_2) at 9.0 L min^{-1}; dry temperature at 200 °C. Ion transfer conditions were: ion funnel RF at 400 Vpp; multiple RF at 200 Vpp; quadrupole low mass at 200 m/z; collision energy at 8.0 eV; collision RF at 2000 Vpp; transfer time at 110.0 μs; pre-pulse storage time at 10.0 μs.

2. Figures.

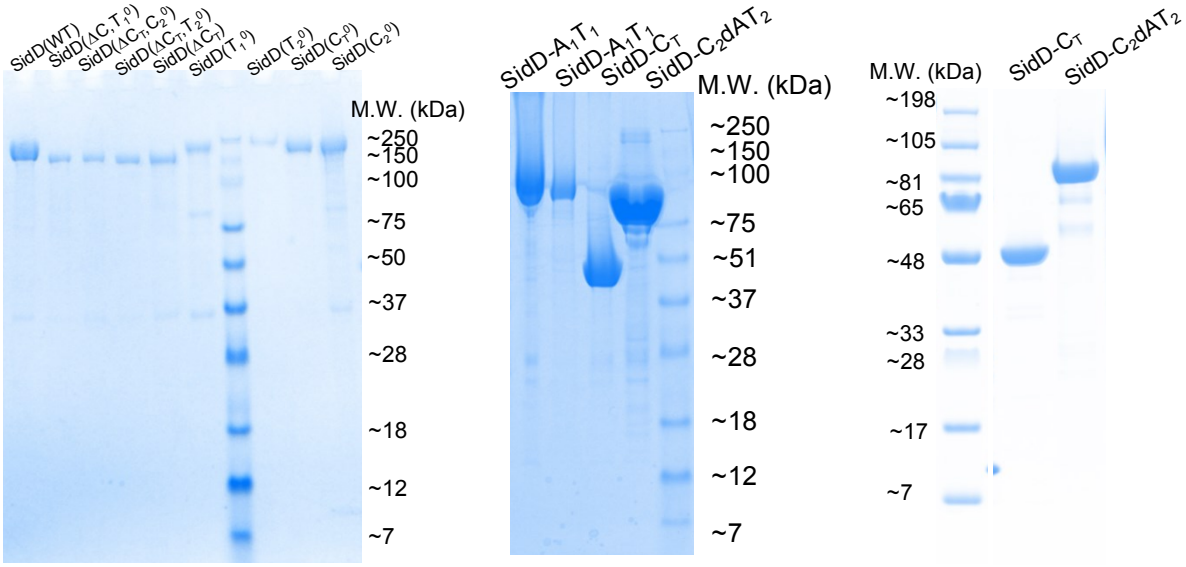

Figure S1. SDS-PAGE analysis of purified SidD and related variants used in this study.

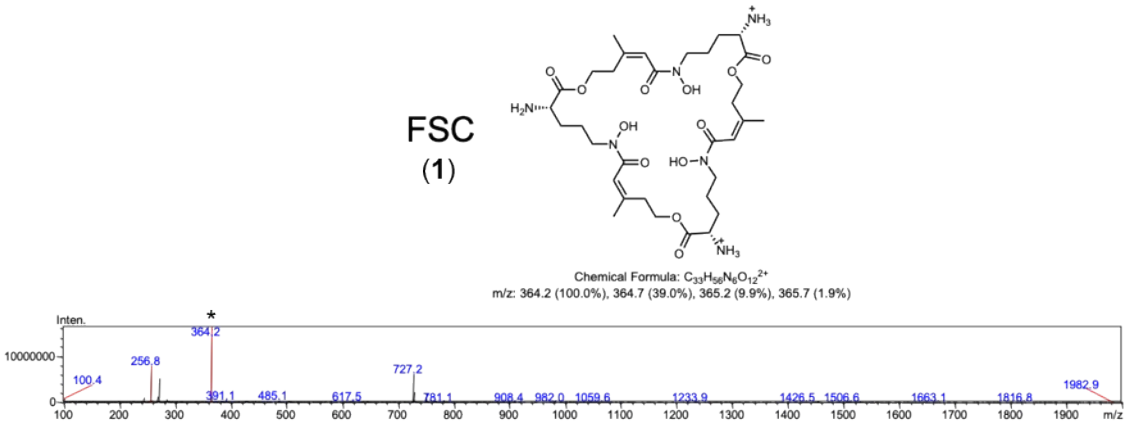

Figure S2. Mass spectrum of FSC (1) from LC-MS analysis of SidD in vitro reaction. The [M+H]+ species is highlighted with an asterisk (*) above the peak.

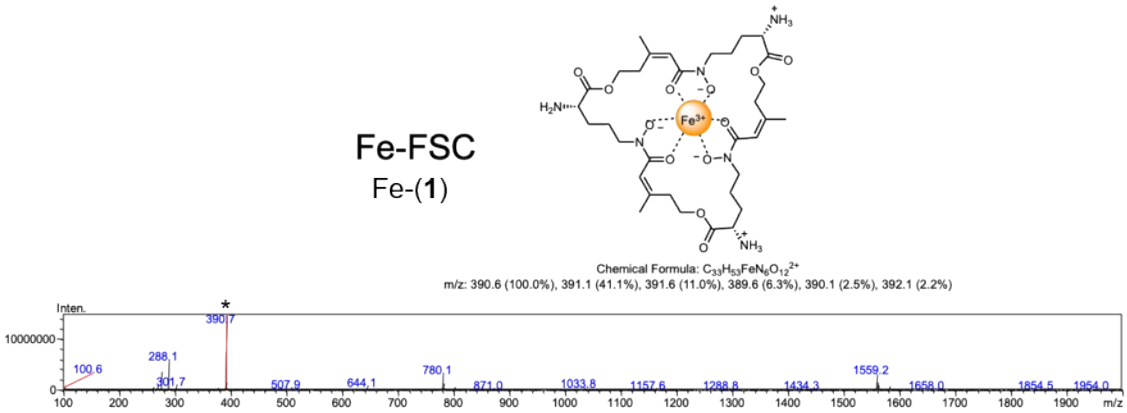

Figure S3. Mass spectrum of Fe-FSC Fe-(1) from LC-MS analysis of SidD in vitro reaction. The [M+H]+ species is highlighted with an asterisk (*) above the peak.

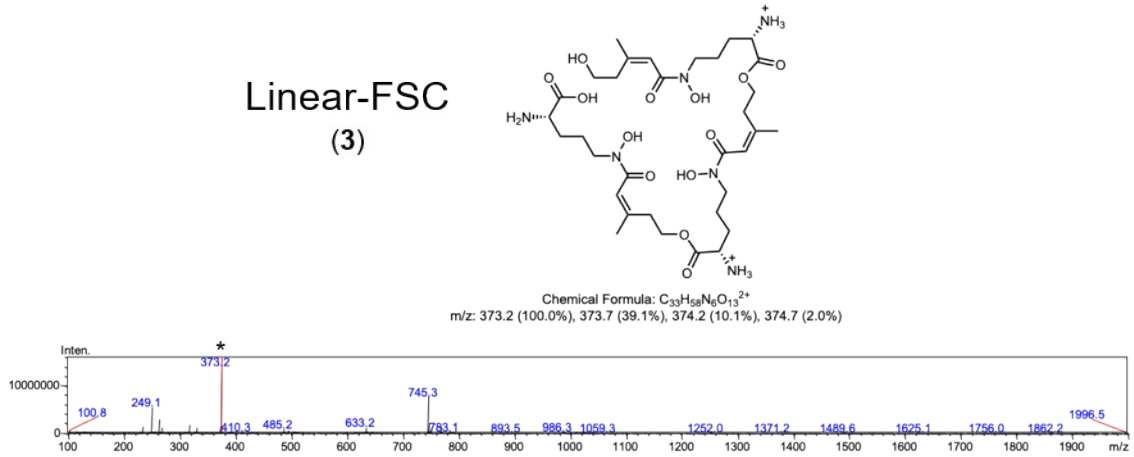

Figure S4. Mass spectrum of Linear-FSC (3) from LC-MS analysis of SidD in vitro reaction. The [M+H]+ species is highlighted with an asterisk (*) above the peak.

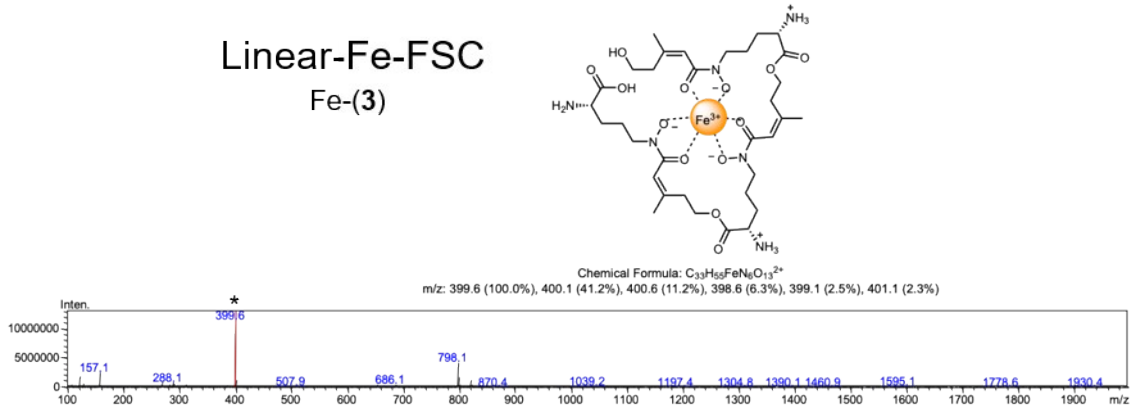

Figure S5. Mass spectrum of Linear-Fe-FSC Fe-(**3**) from LC-MS analysis of SidD *in vitro* reaction. The $[M+H]^+$ species is highlighted with an asterisk (*) above the peak.

Tetra-*cis*-AMHO
(**4**)

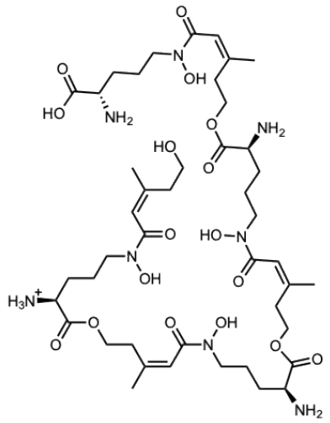

Chemical Formula: $C_{44}H_{75}N_8O_{17}^+$
m/z: 987.5245 (100.0%), 988.5279 (47.6%), 989.5312 (11.1%), 989.5288 (3.5%), 988.5216 (3.0%), 990.5346 (1.7%), 990.5321 (1.7%), 989.5249 (1.4%)

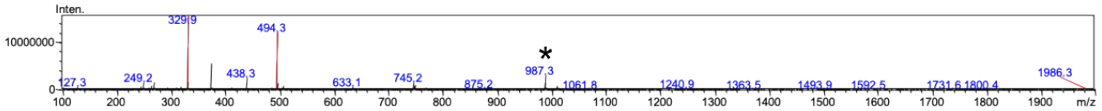

Figure S6. Mass spectrum of tetra-*cis*-AMHO (**4**) from LC-MS analysis of SidD *in vitro* reaction. The $[M+H]^+$ species is highlighted with an asterisk (*) above the peak.

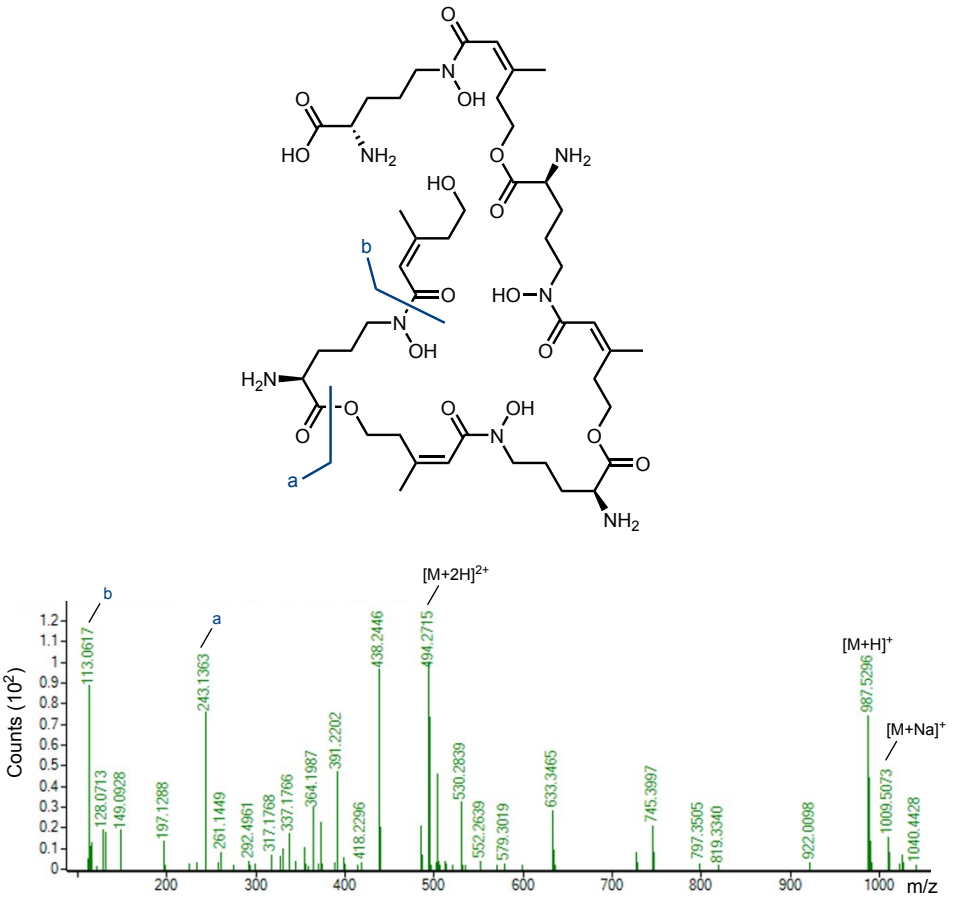

Figure S7. High resolution MS/MS mass spectrum of tetra-*cis*-AMHO (**4**) from LC-MS analysis of SidD *in vitro* reaction.
The $[M+H]^+$, $[M+Na]^+$ and $[M+2H]^{2+}$ species are annotated in addition to fragmentations highlighted on both the structure and spectrum.

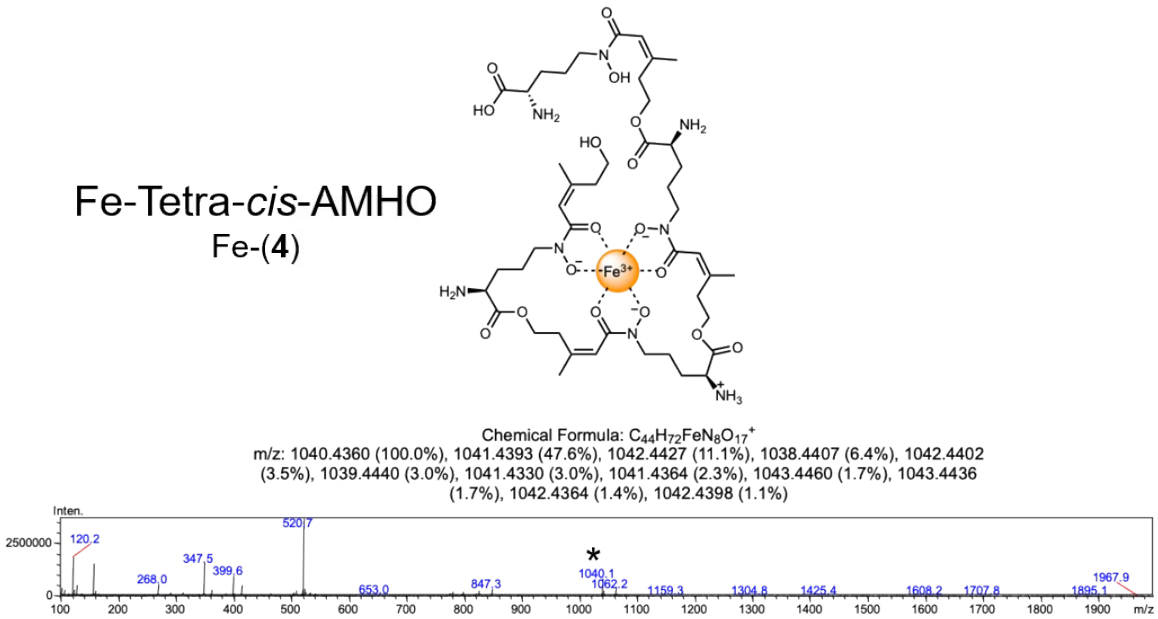

Figure S8. Mass spectrum of Fe-tetra-*cis*-AMHO Fe-(**4**) from LC-MS analysis of SidD *in vitro* reaction.
The $[M+H]^+$ species is highlighted with an asterisk (*) above the peak.

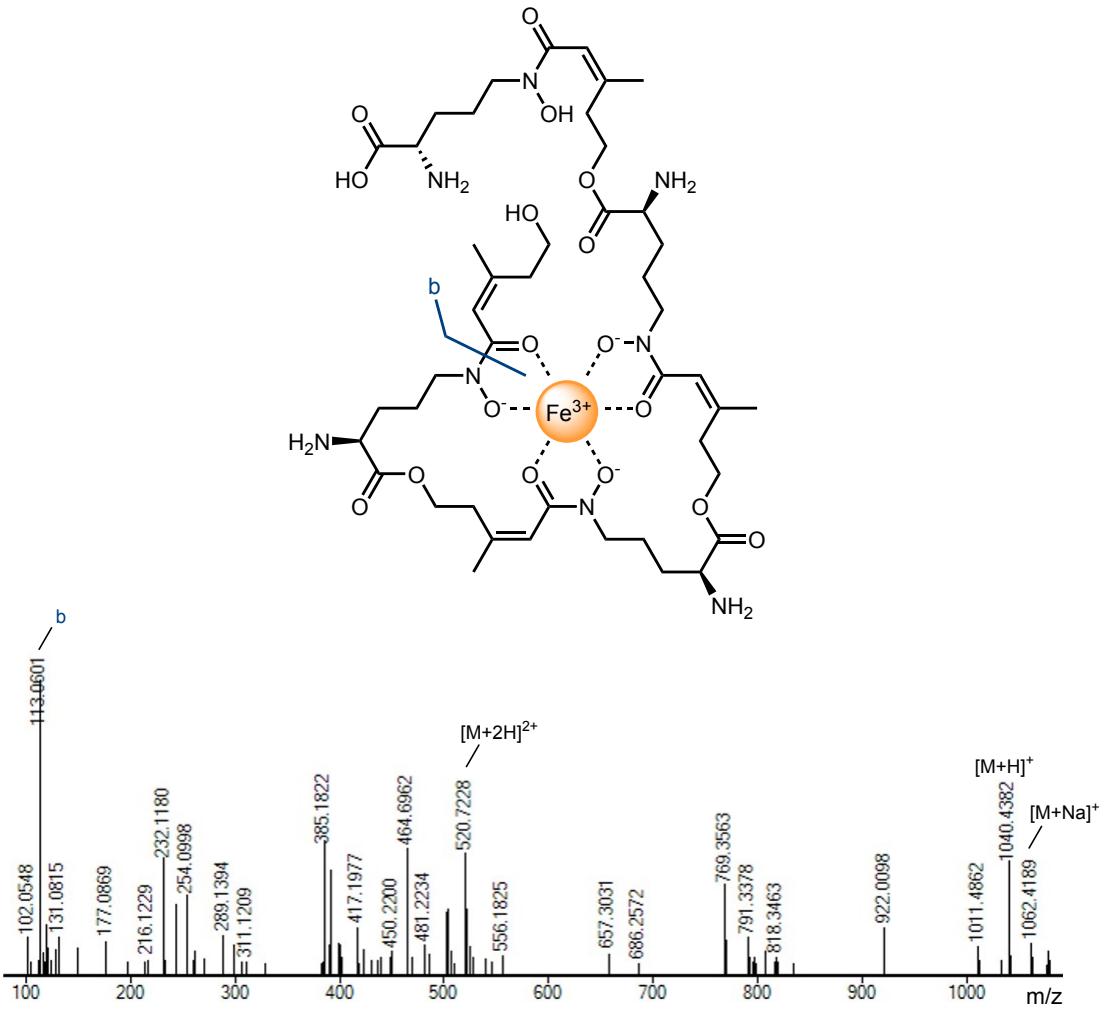

Figure S9. High resolution MS/MS mass spectrum of Fe-tetra-*cis*-AMHO (**4**) from LC-MS analysis of SidD *in vitro* reaction.
The $[M+H]^+$, $[M+Na]^+$ and $[M+2H]^{2+}$ species are annotated in addition to fragmentations highlighted on both the structure and spectrum.

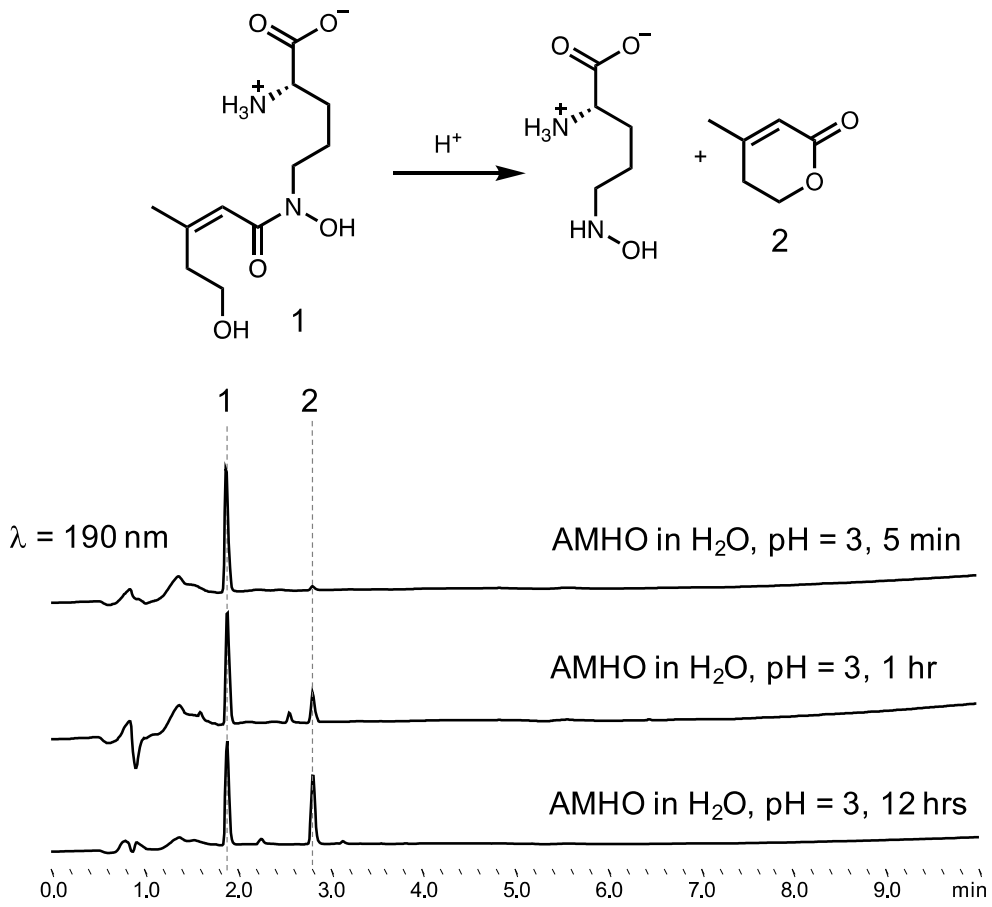

Figure S10. HPLC traces showing degradation of AMHO (1) to N^5-hydroxy-L-ornithine and Δ^2-anhydro-mevalonate lactone (**2**) under acidic conditions.

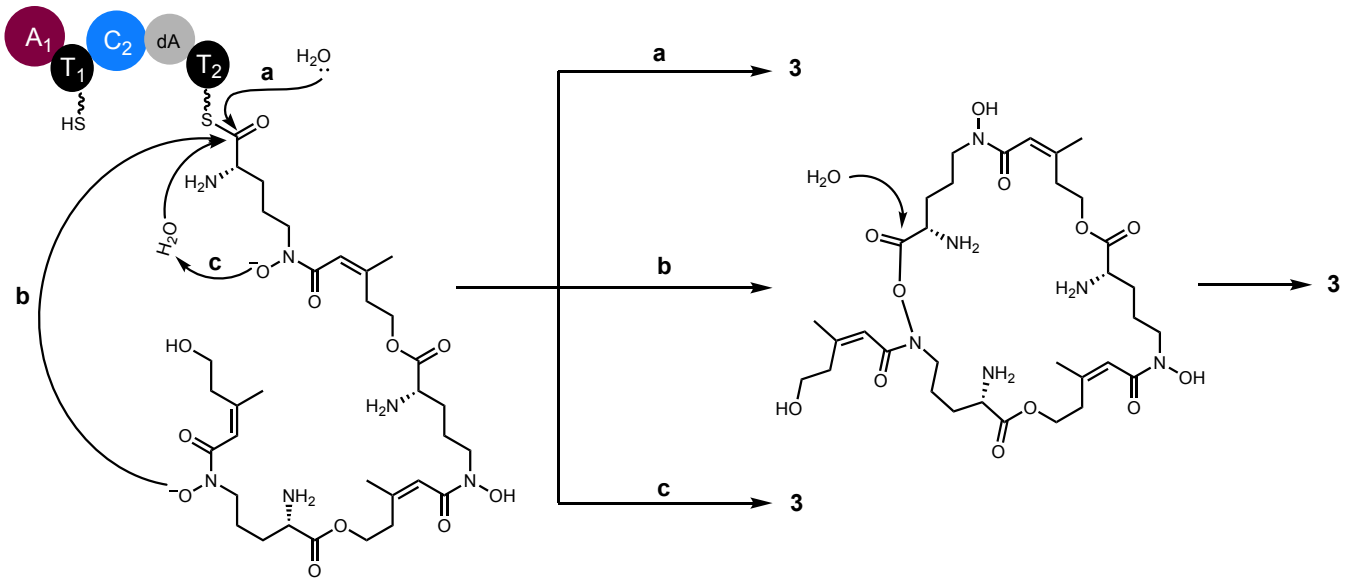

Figure S11. Possible mechanisms for spontaneous intermediate offloading to give **3**.
The observation that, in the presence of Fe^{3+}, hydrolyzed intermediate **3** is not detected suggests direct hydrolysis by water (route a) is slow while a free-hydroxamate group could promote cleavage of thioester either through a non-enzymatic intramolecular nucleophilic attack on the carbonyl of the thioester (route b), or act as a general base (route c). The shunt product **4** could be generated in a similar way.

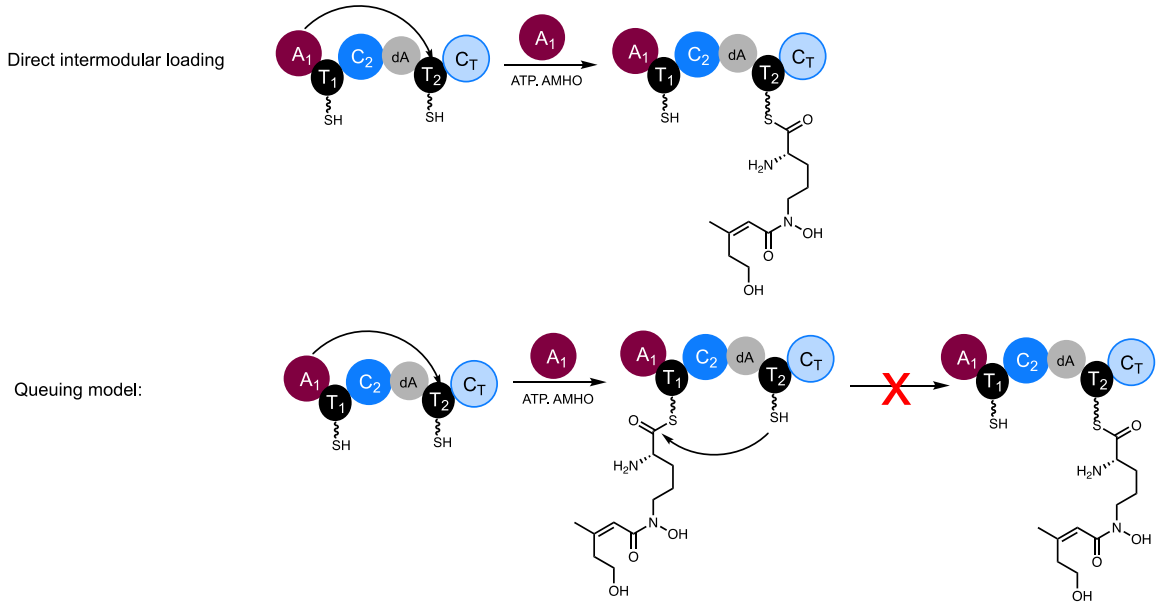

Figure S12. Plausible mechanisms for intermodular T domain loading.
As discussed in the main text, a queuing model is disproved since loading of T_2 is T_1-independent.

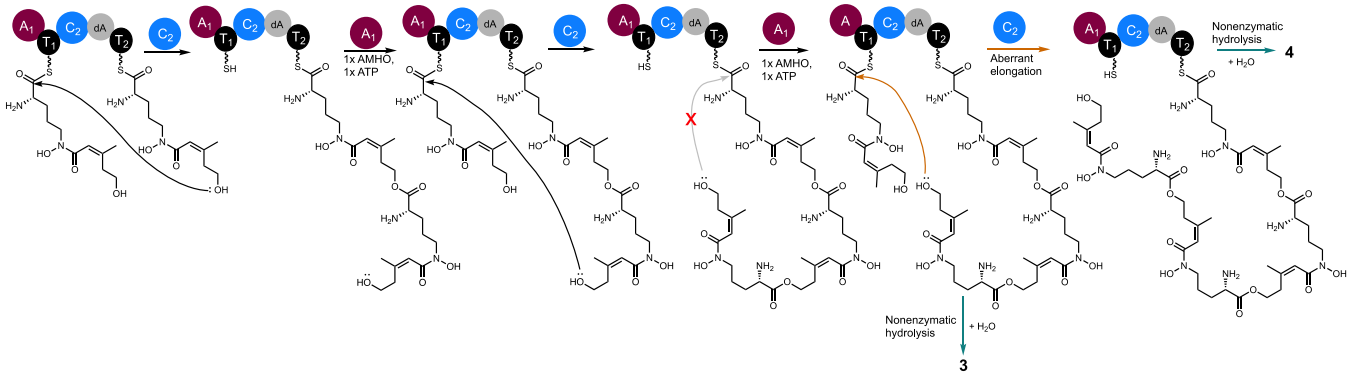

Figure S13. Biosynthetic assembly of *cis*-AMHO units by SidD(ΔC_T).

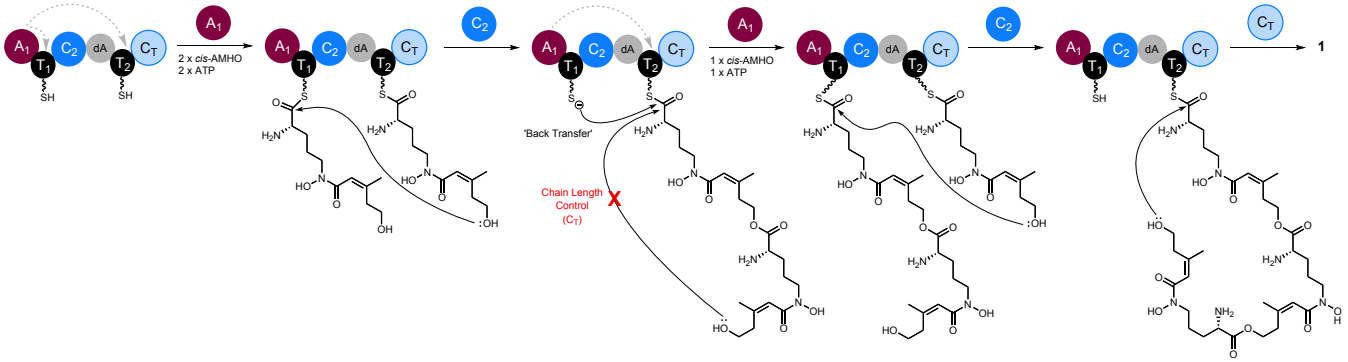

Figure S14. Proposed biosynthetic route to FSC (1) using the 'back transfer' approach.

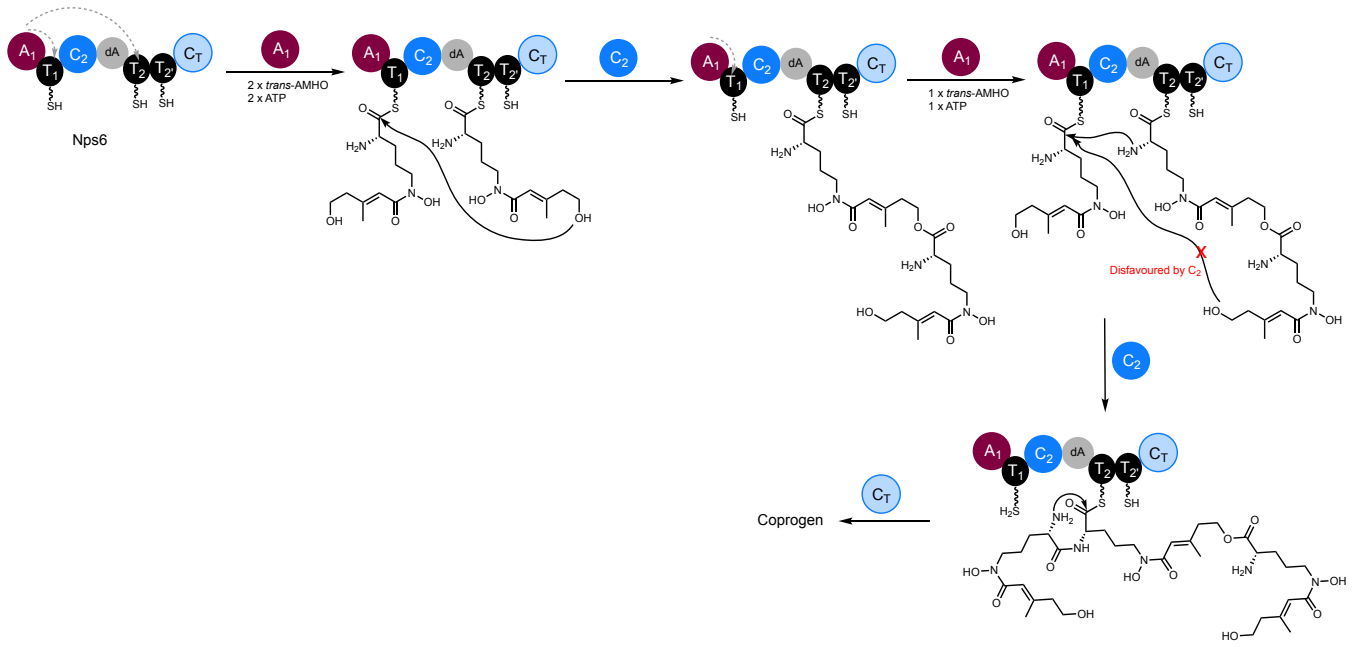

Figure S15. Proposed biosynthetic pathway for coprogen.
For clarity, the intermediates on $T_{2'}$ are not shown. $T_{2'}$ is proposed to work in parallel to T_2 to increase the overall flux of the assembly line.

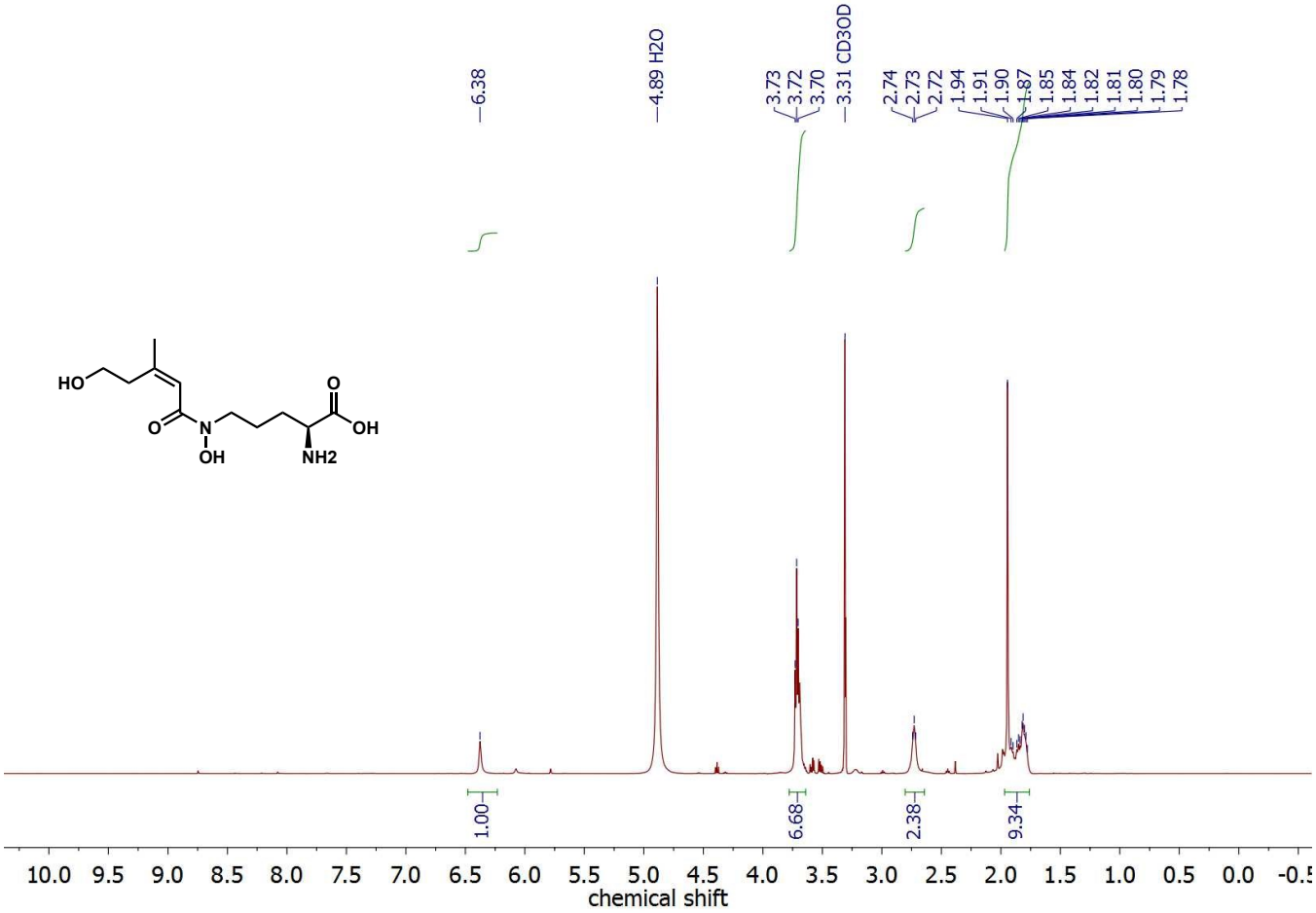

Figure S16. ^{1}H-NMR spectrum of AMHO in CD_3OD.

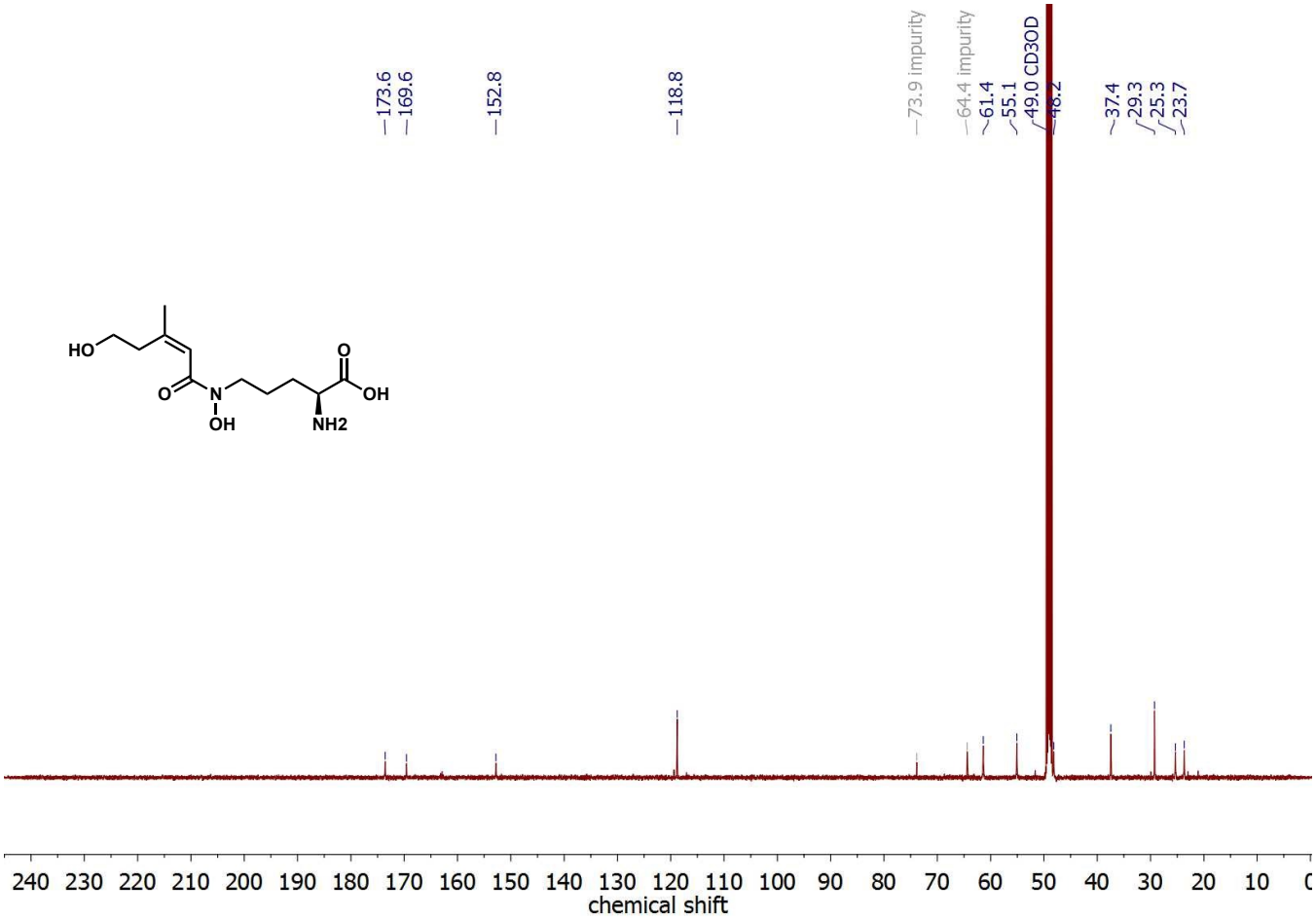

Figure S17. ^{13}C-NMR spectrum of AMHO in CD_3OD.

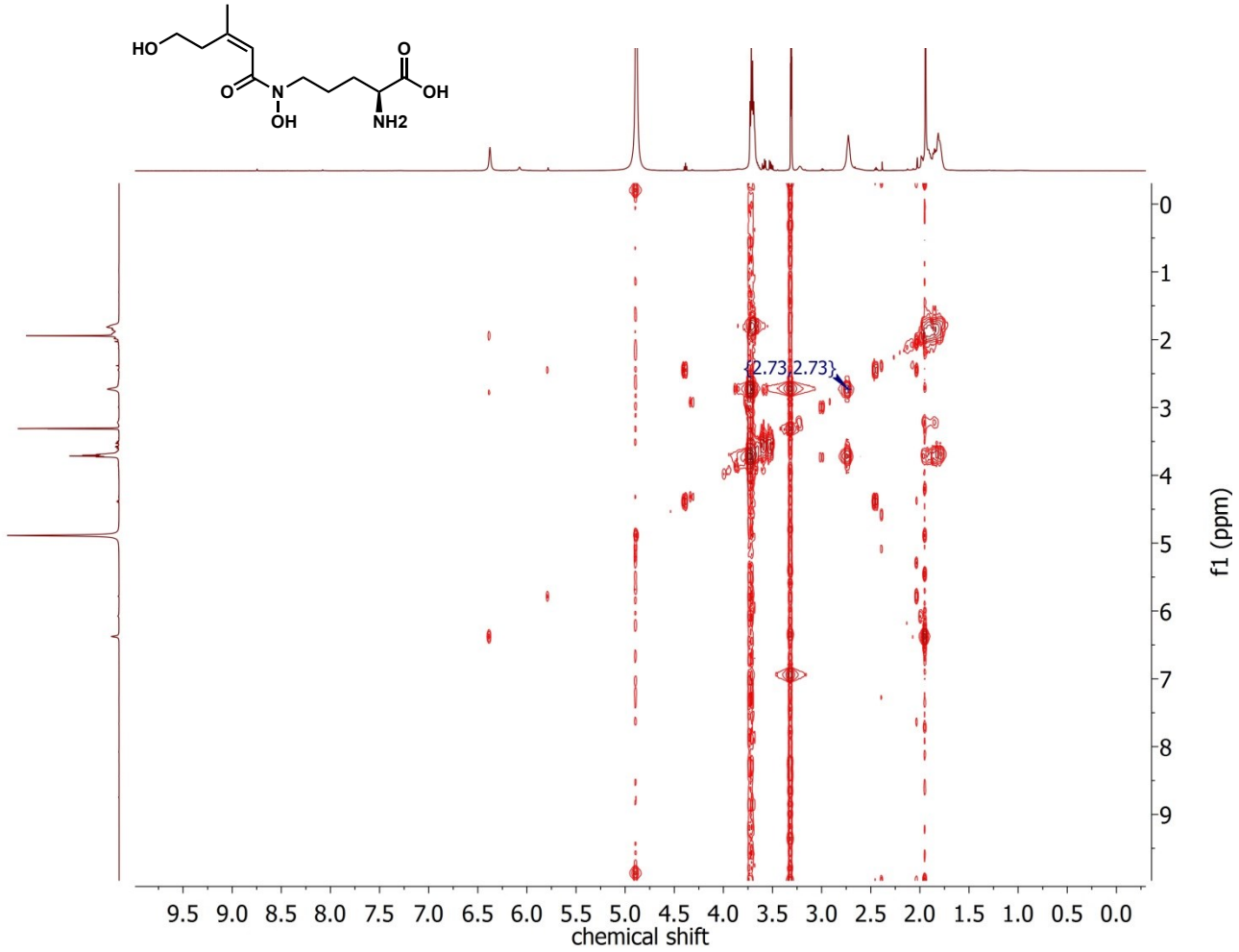

Figure S18. ^{1}H-^{1}H COSY-NMR spectrum of AMHO in CD_3OD.

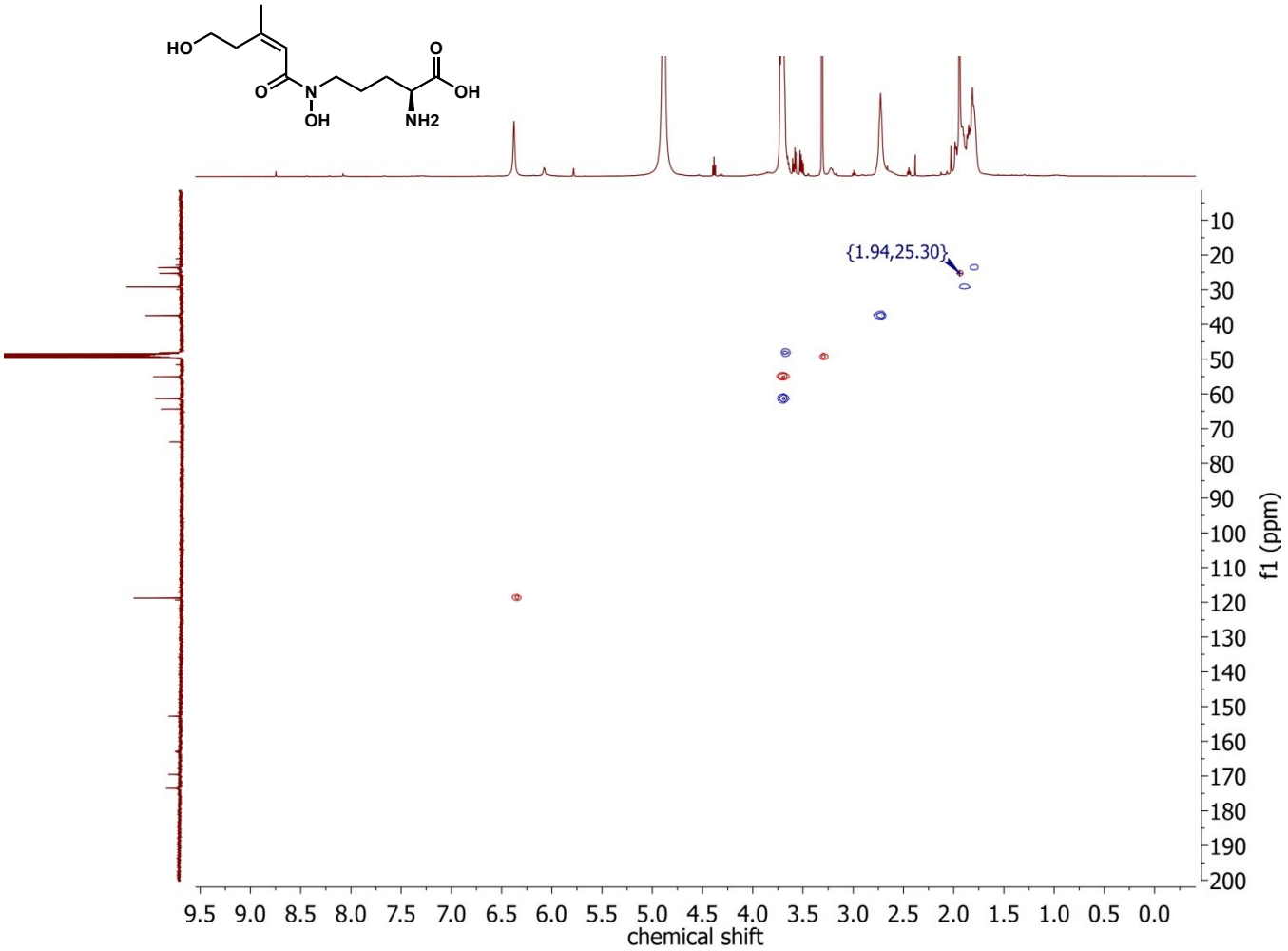

Figure S19. HSQC-NMR spectrum of AMHO in CD_3OD.

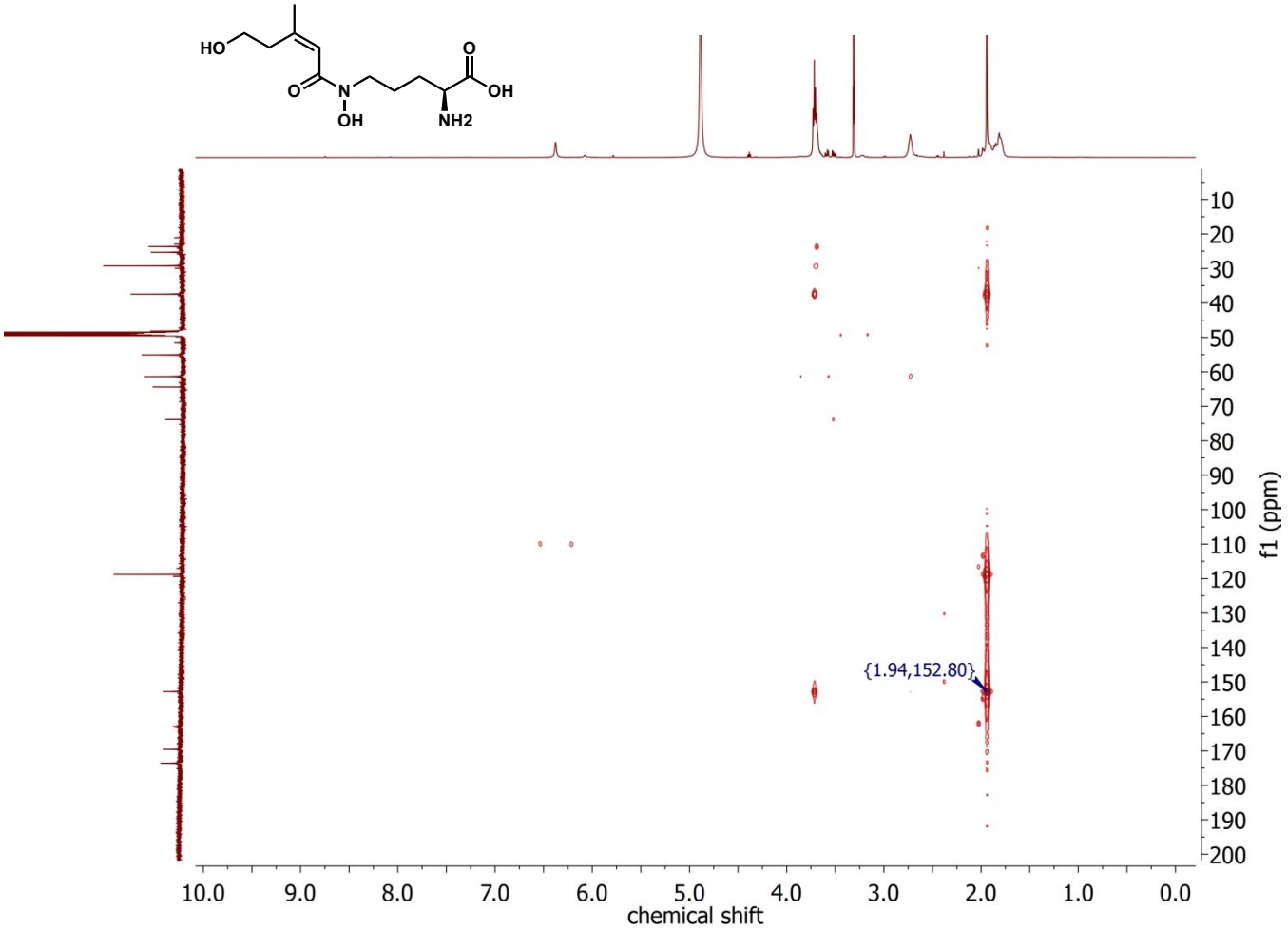

Figure S20. HMBC-NMR spectrum of AMHO in CD_3OD.

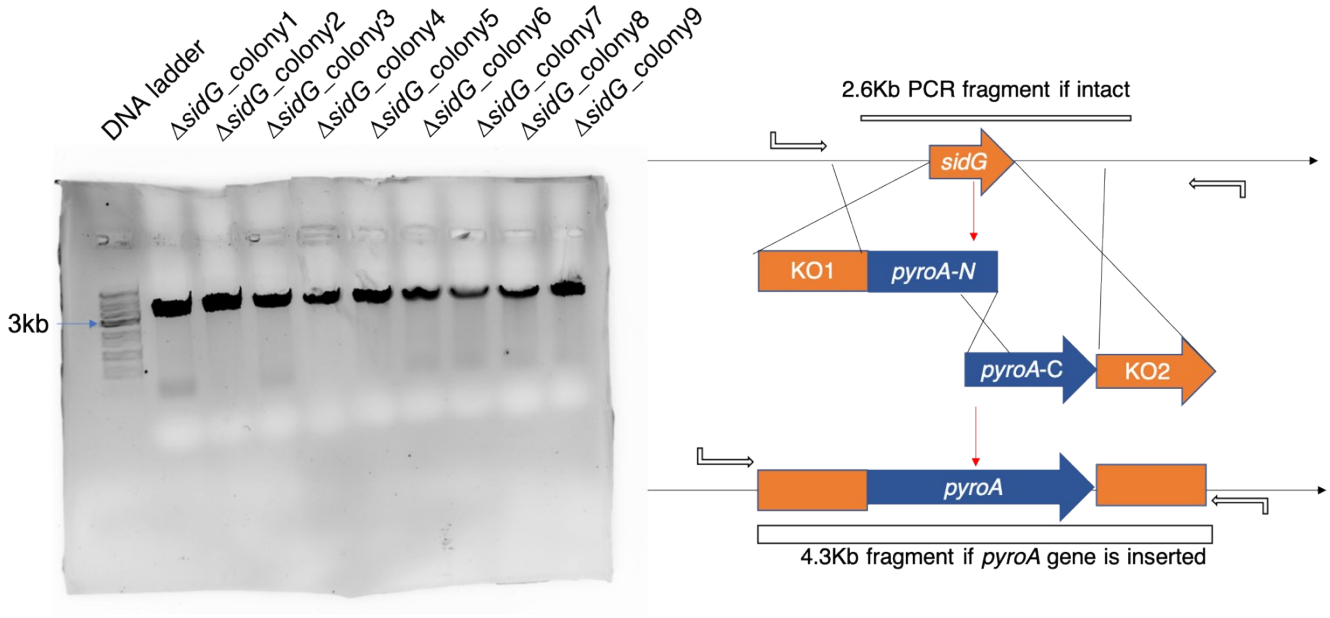

Figure S21. Gene-knockout of *sidG* in *A. nidulans*.
Replacement of *sidG* gene by *pyroA* marker. Successful gene replacement will cause size change of PCR fragments from 2.6 kb to 4.3 kb.

3. Tables

Table S1. Plasmid maps of wild-type constructs used in this study.

Name	Plasmid map
xw55-SidD	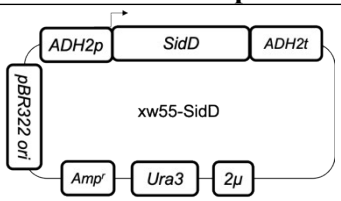
pET28-SidD-A_1T_1	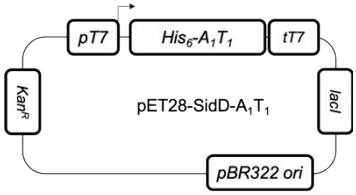
pET28-SidD-C_2dAT_2	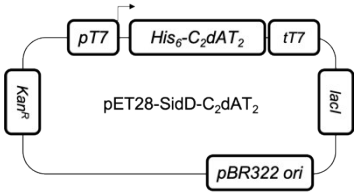
pET28-SidD-C_T	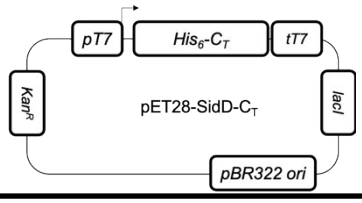

Table S2. Oligonucleotides used for cloning and mutagenesis in this study.

Name	Sequence (5'-3')
SidD-xw55-F1	ATGGCTAGCCATCACCATCACCATCACCATCACACTGGTTCAATACAGCAAGATGAC
SidD-xw55-R1	GATTTCTAGGTGAAGTAACCCTTCATCTTTTGCTTCGTCTG
SidD-xw55-F2	CAGACGAAGCAAAAGATGAAGGGTTACTTCACCTAGAAATC
SidD-xw55-R2	AAATCGTGAAGGCATCGGTCCGCACAAATTTGTCATTTTCACTGTCCACTAAACAACTTG
SidD-H1802A-xw55-F	CATCGGCTTATCCGCCGCCCAATACGATGGCGTCTC
SidD-H1802A-xw55-R	CATCGTATTGGGCGGCGGATAAGCCGATGACGAGGCAG
SidD-ΔC_T-xw55-R	GATAATGAAAACTATAAATCGTGAAGGCATTCATGAGCGTTCATCCACCTTCATC
SidD-A_1T_1-xw55-R	GATAATGAAAACTATAAATCGTGAAGGCATTCATGAGCGTTCATCCACCTTCATC
SidD-ΔC_T-xw55-F	GATAATGAAAACTATAAATCGTGAAGGCATTCATGAGCGTTCATCCACCTTCATC
SidD-S1594A-xw55-F	GCGGTGGTGATGCCGTACTTGCAATGAAG
SidD-S1594A-xw55-R	CAAGTACGGCATCACCACCGCGCCGGAAG
SidD-H999A-xw55-F	GATACATGGTTTGGACTATTCACGCTGTGTTGTACGATGGGTGGTCAG
SidD-H999A-xw55-R	CTGACCACCCATCGTACAACACAGCGTGAATAGTCCAAACCATGTATC
SidD-S801A-xw55-F	CTCTTGGTGGAGACGCCCTCACAGCCATGAAGCTG
SidD-S801A-xw55-R	CTTCATGGCTGTGAGGGCGTCTCCACCAAGAGCGAAG
SidD-C_T-pET28-F	CACCATGAAAACCTGTACTTCCAATCCAATTCATATCAGCCGTTTTCGATGCTCCGTC
SidD-C_T-pET28-R	GAATTCGGATCCGTTATCCACTTCCAATTCACTGTCCACTAAACAACTTGCTATCCAGC
SidD-A_1T_1-pET28-F	CACCATGAAAACCTGTACTTCCAATCCAATGGTTCAATACAGCAAGATGACGTTCACAAT
SidD-A_1T_1-pET28-R	TTCGGATCCGTTATCCACTTCCAATttaGTCGACGTCGCAAATACGGACAACG
SidD-T_2-pET28-F	ACCTGTACTTCCAATCCAATTCAGCTTCAGAAAGCATTCTGCGGTC
SidD-T_2-pET28-R	GATCCGTTATCCACTTCCAATTCATGAGCGTTCATCCACCTTCATC
SidD-C_2dAT_2-pET28-F	CACCATGAAAACCTGTACTTCCAATCCAATGACGTGCAAAGGACAGTCCCGGCATTCTCG
SidD-C_2dAT_2-pET28-R	GATCCGTTATCCACTTCCAATTCATGAGCGTTCATCCACCTTCATC
SidG-KOcassette1-F	CAATCAACTATCAACTATTAACTATATCGTAATACGGGCTGCTGGCATGTCAC
SidG-KOcassette1-R	CTGACAGCGCCATAAGACAAGGTGAACTGGCGGTGGGGGTGGTAG
SidG-KOpyroA-F	CACCGCCAGTTCACCTTGTCTTATGGCGCTGTCAGGGTGTGTATTCAAG
SidG-KOpyroA-R	GTAGTTTTTTTGACCTTTATCCCCTGGTATCATGGTTGTTGGGTC
SidG-KOcassette2-F	CAACCATGATACCAGGGGATAAAGGTCAAAAAAACTACTTTCATATAAAAAACATG
SidG-KOcassette2-R	CATACTTGATAATGAAAACTATAAATCGTGAAGGCATCTATTCCTCCTTCTCTGCATC
SidG-KOsplit-pyroA-N-F	GGGCTGCTGGCATGTCACCCTTG
SidG-KOsplit-pyroA-N-R	CTGTCATGGCCAAAGCTCGTATCGG
SidG-KOsplit-pyroA-C-F	GAACACTCCGTCGCAGCCCAG
SidG-KOsplit-pyroA-C-R	CTATTCCTCCTTCTCTGCATCCGACCAAG

SidG-KOcheckF	GCCTGTGTATCGATACTAGCGCACG
SidG-KOcheckR	CAATAAACTCCTGACACCGGACTTTATG

Table S3. ^{1}H and ^{13}C NMR chemical shifts of AMHO measured in CD_3OD. The numbered structure of AMHO is shown for reference.

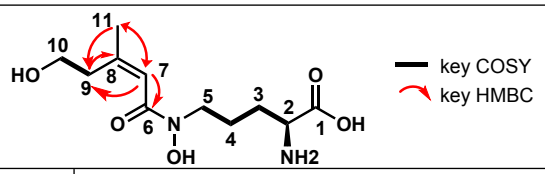

Pos.	δ_C (CD_3OD)	δ_H (CD_3OD), multi, *J*, integration
1	173.6, C	–
2	55.1, CH_3	3.72, t, *J* = 6.4 Hz, 1H
3	29.3, CH_2	1.90-1.78, m, overlap, 2H
4	23.7, CH_2	1.88-1.76, m, overlap, 2H
5	48.2, CH_2	3.70, t, overlap, 2H
6	169.6,C	–
7	118.8, CH	6.38, s, 1H
8	152.8, C	–
9	37.4, CH_2	2.73, t, *J* = 6.6 Hz, 2H
10	61.4, CH_2	3.70, t, overlap, 2H
11	25.3, CH_3	1.94, s, 3H

Table S4. Amino acid sequences of wild-type SidD protein and other SidD constructs used in this study**.**

Name	Sequence (5'-3')
SidD	MASHHHHHHHHTGSIQQDDVHNQIDHCNQSDDLPAARLNCNDVELFEVAGLACDETSSPTGMRDE MVLLSWLIALLRTREGGQIRYEWAYRYPEEEPVPRCLAMNEVVAGLQSSVKETAAAVSRHISADVSS PPAPASLLLSTSSLSQTSDEAKDEGLLHLEIAFENGLCKIRPTWHSENMLPFTVTRYARTLIDTVRLCV SNCDAAIQDCLRPTAYDLDEIWRWNHNLPPTYNFCMHEIISDQAQKFPDKEAIASWDGSLTYRQIDQ YSSFVARSLIGMGVGLHDVLPVCFEKSRWTIVAVLAVMKAGATFVLMDPTLPLARLQNMAQQVGA KMMVSSRGQYNLATEIIPNANVLVVEENTFSSLSAEQNGEPLPTVPSSALMYMIFTSGSTGTPKGVKIS HETYTSSAIPRANAVGYTEDSRVLDFASYAFDVSIDSMLLTLGNGGCLCIPSDEDRLNDINGVIRRMK VNYAGLTPSVARILDADVISSLSGLGLGGEAVSARDVNLWGQDTRIIIGYGPCECTIGCTVNSSAATG RDYISIGPGNGAVIWIVDPNDHESLVPLGAVGELLVEGPIVGQGYLNDPEKTAAAFIEDPSWLVAGHE GYPGRRGRLYKTGDLGRYDPDGSGGIVFVGRKDTQVKLRGQRVELGEIESQLRARLPSETTVIAEVIV PQGSGGQPTLVAFVAAQTTKGHDHTGLEAAELPDELRRALSEADAELAKVLPRYMVPTAYIPVNHIP TLISGKTDRKRLRQFGATVDLRQLDQDATNTAARELSDLERRLRQAWSQTLKLQACSIRLQDNFFAL GGDSLTAMKLVSVCRSQGLDLSVTSMFSNPTLSAMASVVRICDVDVQRTVPAFSMITSDMNSACVE AAEPCGVGPADIEDIYPCTPTQESLFTFSLKSVKPYVAQRVLCIPSHIDLNAWRKAWEDVVAALPILRT RVAQLQEPGLQQVVLKNSISWTQASDLAEYLENDRTQKMNLGESLARYAIVEDSADGKRYMVWTI HHVLYDGWSEPIILKQVSDALQGQPVEVKAQMRDFVRFVRDSDDAAVQEFWRRELKGAVGPQFPRL PSRDFMPTPDALVERQVSLDTSSGSPFTMATLIRGAWALVASQYTGSDDIVFGETLTGRDIPLPGVESI VGPLIATVPIRVRILRGSTVESYLQAVQQSVLARTPYQHLGMQNIRKVSQDAQHACETGTGLVIQPEP EYVGSELGVERGDVVLEALHFNPYPLMLACGIRKGGFRVCASFDSSLIETRQMERMLAQLETACWQ LSQGLSRKVDEISCLPEAELNQIWQWNRSPPLSLDETTSRLRANASTKPGSSYPPAVVPWVCSPRNSS LLSPIGCVGELWLEGALLSGDTVDSPAWLVAGSSTCAGRTGKVQATGDMVQLREDGSLVFVGRKEN VVPVQGHAVDITEIERHLAEHLPPTIRAAATVVRSSSDQELVMFIEQPAAEEACIELLSEKREIVCDAP DKAFQTTICATIPGSLAAVLKKLDKYMRDSLPSYMAPSAYIVVEKLPNTMDDIDHNLLNQIASQVTPQ ILNELRDGLSNAWTKATAPNHLSASESILRSAWAKVLRVDPEQIDVDDNFFRRGGDSVLAMKLVSSL RAQGYSLSVADIFRHMRLSDAARVMKVDERSTEKINSYQPFSMLRLPDVQQFLANIVRPQLGDQHW PIRDVLPVTDSQDMDIRATIQPPRTSIQYTMLYFDNSVDRERLFRSCSDLVKTHEILRTVFISHESSFLQ VVLNELEIPVRAHKTDKQLDQYVASLFREDIESNFQLGCPFLRLFYVEGNNGESCLVIGLSHAQYDGV SLPRLLQDLDALYTGTQLATFSPFSLYMAQTSEEAIQNKAAAYWRNLLSSSSLSTLDGPSSDPTDKAIF HTRPVNIHPLKEITTANLLTAAWAMVLARRLQTPDVTFGSVTSGRTLDIPNAENFMGPCYQLTPVRVP FHPDWTASDLLNFVQTQSAESAAHDFLGFEKIAKLAGWASGRQGFDSIVHHQDWEDFDMMPFGGGS CRVDIANPHGDAAYPVKAVSFVKEGEIHVGVVGSERDVMFVDEVLGELAAAVVELAGQSTEVLLDS KLFSGQ*
SidD(ΔC_T)	MASHHHHHHHHTGSIQQDDVHNQIDHCNQSDDLPAARLNCNDVELFEVAGLACDETSSPTGMRDE MVLLSWLIALLRTREGGQIRYEWAYRYPEEEPVPRCLAMNEVVAGLQSSVKETAAAVSRHISADVSS PPAPASLLLSTSSLSQTSDEAKDEGLLHLEIAFENGLCKIRPTWHSENMLPFTVTRYARTLIDTVRLCV

	SNCDAAIQDCLRPTAYDLDEIWRWNHNLPPTYNFCMHEIISDQAQKFPDKEAIASWDGSLTYRQIDQ YSSFVARSLIGMGVGLHDVLPVCFEKSRWTIVAVLAVMKAGATFVLMDPTLPLARLQNMAQQVGA KMMVSSRGQYNLATEIIPNANVLVVEENTFSSLSAEQNGEPLPTVPSSALMYMIFTSGSTGTPKGVKIS HETYTSSAIPRANAVGYTEDSRVLDFASYAFDVSIDSMLLTLGNGGCLCIPSDEDRLNDINGVIRRMK VNYAGLTPSVARILDADVISSLSGLGLGGEAVSARDVNLWGQDTRIIIGYGPCECTIGCTVNSSAATG RDYISIGPGNGAVIWIVDPNDHESLVPLGAVGELLVEGPIVGQGYLNDPEKTAAAFIEDPSWLVAGHE GYPGRRGRLYKTGDLGRYDPDGSGGIVFVGRKDTQVKLRGQRVELGEIESQLRARLPSETTVIAEVIV PQGSGGQPTLVAFVAAQTTKGHDHTGLEAAELPDELRRALSEADAELAKVLPRYMVPTAYIPVNHIP TLISGKTDRKRLRQFGATVDLRQLDQDATNTAARELSDLERRLRQAWSQTLKLQACSIRLQDNFFAL GGDSLTAMKLVSVCRSQGLDLSVTSMFSNPTLSAMASVVRICDVDVQRTVPAFSMITSDMNSACVE AAEPCGVGPADIEDIYPCTPTQESLFTFSLKSVKPYVAQRVLCIPSHIDLNAWRKAWEDVVAALPILRT RVAQLQEPGLQQVVLKNSISWTQASDLAEYLENDRTQKMNLGESLARYAIVEDSADGKRYMVWTI HHVLYDGWSEPIILKQVSDALQGQPVEVKAQMRDFVRFVRDSDDAAVQEFWRRELKGAVGPQFPRL PSRDFMPTPDALVERQVSLDTSSGSPFTMATLIRGAWALVASQYTGSDDIVFGETLTGRDIPLPGVESI VGPLIATVPIRVRILRGSTVESYLQAVQQSVLARTPYQHLGMQNIRKVSQDAQHACETGTGLVIQPEP EYVGSELGVERGDVVLEALHFNPYPLMLACGIRKGGFRVCASFDSSLIETRQMERMLAQLETACWQ LSQGLSRKVDEISCLPEAELNQIWQWNRSPPLSLDETTSRLRANASTKPGSSYPPAVVPWVCSPRNSS LLSPIGCVGELWLEGALLSGDTVDSPAWLVAGSSTCAGRTGKVQATGDMVQLREDGSLVFVGRKEN VVPVQGHAVDITEIERHLAEHLPPTIRAAATVVRSSSDQELVMFIEQPAAEEACIELLSEKREIVCDAP DKAFQTTICATIPGSLAAVLKKLDKYMRDSLPSYMAPSAYIVVEKLPNTMDDIDHNLLNQIASQVTPQ ILNELRDGLSNAWTKATAPNHLSASESILRSAWAKVLRVDPEQIDVDDNFFRRGGDSVLAMKLVSSL RAQGYSLSVADIFRHMRLSDAARVMKVDERS*
SidD-A_1T_1	MASHHHHHHHHTGSIQQDDVHNQIDHCNQSDDLPAARLNCNDVELFEVAGLACDETSSPTGMRDE MVLLSWLIALLRTREGGQIRYEWAYRYPEEEPVPRCLAMNEVVAGLQSSVKETAAAVSRHISADVSS PPAPASLLLSTSSLSQTSDEAKDEGLLHLEIAFENGLCKIRPTWHSENMLPFTVTRYARTLIDTVRLCV SNCDAAIQDCLRPTAYDLDEIWRWNHNLPPTYNFCMHEIISDQAQKFPDKEAIASWDGSLTYRQIDQ YSSFVARSLIGMGVGLHDVLPVCFEKSRWTIVAVLAVMKAGATFVLMDPTLPLARLQNMAQQVGA KMMVSSRGQYNLATEIIPNANVLVVEENTFSSLSAEQNGEPLPTVPSSALMYMIFTSGSTGTPKGVKIS HETYTSSAIPRANAVGYTEDSRVLDFASYAFDVSIDSMLLTLGNGGCLCIPSDEDRLNDINGVIRRMK VNYAGLTPSVARILDADVISSLSGLGLGGEAVSARDVNLWGQDTRIIIGYGPCECTIGCTVNSSAATG RDYISIGPGNGAVIWIVDPNDHESLVPLGAVGELLVEGPIVGQGYLNDPEKTAAAFIEDPSWLVAGHE GYPGRRGRLYKTGDLGRYDPDGSGGIVFVGRKDTQVKLRGQRVELGEIESQLRARLPSETTVIAEVIV PQGSGGQPTLVAFVAAQTTKGHDHTGLEAAELPDELRRALSEADAELAKVLPRYMVPTAYIPVNHIP TLISGKTDRKRLRQFGATVDLRQLDQDATNTAARELSDLERRLRQAWSQTLKLQACSIRLQDNFFAL GGDSLTAMKLVSVCRSQGLDLSVTSMFSNPTLSAMASVVRICDVD*
SidD-C_2T_2	MGSSHHHHHHENLYFQSNDVQRTVPAFSMITSDMNSACVEAAEPCGVGPADIEDIYPCTPTQESLFTF SLKSVKPYVAQRVLCIPSHIDLNAWRKAWEDVVAALPILRTRVAQLQEPGLQQVVLKNSISWTQASD

	LAEYLENDRTQKMNLGESLARYAIVEDSADGKRYMVWTIHHVLYDGWSEPIILKQVSDALQGQPVE VKAQMRDFVRFVRDSDDAAVQEFWRRELKGAVGPQFPRLPSRDFMPTPDALVERQVSLDTSSGSPF TMATLIRGAWALVASQYTGSDDIVFGETLTGRDIPLPGVESIVGPLIATVPIRVRILRGSTVESYLQAV QQSVLARTPYQHLGMQNIRKVSQDAQHACETGTGLVIQPEPEYVGSELGVERGDVVLEALHFNPYPL MLACGIRKGGFRVCASFDSSLIETRQMERMLAQLETACWQLSQGLSRKVDEISCLPEAELNQIWQWN RSPPLSLDETTSRLRANASTKPGSSYPPAVVPWVCSPRNSSLLSPIGCVGELWLEGALLSGDTVDSPA WLVAGSSTCAGRTGKVQATGDMVQLREDGSLVFVGRKENVVPVQGHAVDITEIERHLAEHLPPTIR AAATVVRSSSDQELVMFIEQPAAEEACIELLSEKREIVCDAPDKAFQTTICATIPGSLAAVLKKLDKY MRDSLPSYMAPSAYIVVEKLPNTMDDIDHNLLNQIASQVTPQILNELRDGLSNAWTKATAPNHLSAS ESILRSAWAKVLRVDPEQIDVDDNFFRRGGDSVLAMKLVSSLRAQGYSLSVADIFRHMRLSDAARV MKVDERS*
SidD-C_T	MGSSHHHHHHENLYFQSNSYQPFSMLRLPDVQQFLANIVRPQLGDQHWPIRDVLPVTDSQDMDIRA TIQPPRTSIQYTMLYFDNSVDRERLFRSCSDLVKTHEILRTVFISHESSFLQVVLNELEIPVRAHKTDKQ LDQYVASLFREDIESNFQLGCPFLRLFYVEGNNGESCLVIGLSHAQYDGVSLPRLLQDLDALYTGTQL ATFSPFSLYMAQTSEEAIQNKAAAYWRNLLSSSSLSTLDGPSSDPTDKAIFHTRPVNIHPLKEITTANLL TAAWAMVLARRLQTPDVTFGSVTSGRTLDIPNAENFMGPCYQLTPVRVPFHPDWTASDLLNFVQTQ SAESAAHDFLGFEKIAKLAGWASGRQGFDSIVHHQDWEDFDMMPFGGGSCRVDIANPHGDAAYPV KAVSFVKEGEIHVGVVGSERDVMFVDEVLGELAAAVVELAGQSTEVLLDSKLFSGQ*

Table S5. Calculated and measured mass values for species detected using intact protein mass spectrometry.

Species	Mass Calculated (Da)	Mass Measured (Da)
apo-SidD(ΔC_T)	179,930	179,946
holo-SidD(ΔC_T)	180,610	180,626
holo-SidD(ΔC_T)-1xAMHO (Intermediate I)	180,852	180,867
holo-SidD(ΔC_T)-4xAMHO-Fe^{3+} (Intermediate IV)	181,631	181,651
holo-SidD-C_2dAT_2	89,815	89,816
holo-C_2dAT_2-3xAMHO-Fe^{3+}	90,594	90,588
apo-SidD(ΔC_T, C_2^0)	179,864	179,881
holo-SidD(ΔC_T, C_2^0)	180,544	180,562
holo-SidD(ΔC_T, C_2^0)-1xAMHO (Intermediate I)	180,786	180,806
holo-SidD(ΔC_T, C_2^0)-2xAMHO (Intermediate II)	181,028	181,047
apo-SidD(ΔC_T, T_1^0)	179,914	179,934
holo- SidD(ΔC_T, T_1^0)	180,254	180,274

References

1. Lin, H.-C.; Chooi, Y.-H.; Dhingra, S.; Xu, W.; Calvo, A. M.; and Tang, Y. (2013) The fumagillin biosynthetic gene cluster in *Aspergillus fumigatus* encodes a cryptic terpene cyclase involved in the formation of β-*trans*-bergamotene. *J. Am. Chem. Soc.* 135, 12, 4616-4619
2. Liu, N.; Hung, Y.-S.; Gao, S.-S.; Hang, L.; Zou, Y.; Chooi, Y.-H.; and Tang, Y. (2017) Identification and heterologous production of a benzoyl-primed tricarboxylic acid polyketide intermediate form the Zaragozic acid A biosynthetic pathway. *Org. Lett.* 2017, 19, 13, 3560-3563.
3. Eisendle, M.; Schrettl, M.; Kragl, C.; Müller, D.; Illmer, P.; and Haas, H. (2006) The intracellular siderophore ferricrocin is involved in iron storage, oxidative-stress resistance, germination, and sexual development in *Aspergillus nidulans*. *Eukaryot. Cell* 5, 1596-1603.
4. Jalal, M.A.; Love, S.K.; and van der Helm, D. (1986) Siderophore mediated iron(III) uptake in *Gliocladium virens*. 1. Properties of *cis*-fusarinine, *trans*-fusarinine, dimerum acid, and their ferric complexes. *J. Inorg. Biochem.* 24, 417-430.